

Investigating the clinical potential of Quantitative Susceptibility Mapping (QSM) - initial results in pediatric patients

Ferdinand Schweser¹, Martin Stenzel², Andreas Deistung¹, Karsten Sommer¹, Hans-Joachim Mentzel², and Jürgen Rainer Reichenbach¹

¹Medical Physics Group, Dept. of Diagnostic and Interventional Radiology I, Jena University Hospital, Jena, Germany, ²Section Pediatric Radiology, Dept. of Diagnostic and Interventional Radiology I, Jena University Hospital, Jena, Germany

INTRODUCTION – Quantitative susceptibility mapping (QSM) is a novel imaging technique that employs the complex-phase of conventional gradient-echo sequences to obtain quantitative maps of bulk tissue magnetic susceptibility [1]. Several studies have demonstrated recently unprecedented contrast of brain tissue on susceptibility maps, especially at high (≥ 3 Tesla) field strengths (e.g. [2,3]) that is complementary to all other established MRI contrasts. In QSM paramagnetic substances (e.g. deoxyheme and ferritin) appear bright and diamagnetic substances (e.g. calcium and myelin) appear dark [2]. Although QSM is currently regarded as the successor of the well-established Susceptibility Weighted Imaging (SWI) technique [4], only few studies have hitherto investigated the potential of applying QSM to pathologic conditions in a clinical scenario [5], thus impressing the perception of QSM being a research tool only so far. This paper presents initial results of applying QSM in routine pediatric neuroradiology to demonstrate the impressive potential of this novel imaging technique.

MATERIALS AND METHODS – Whole-brain data were acquired from 14 pediatric patients (aged 3 yrs 1 mos to 14 yrs 11 mos, 8 male, 6 female) at 1.5 T using a single-channel receive head coil (Magnetom Sonata and Magnetom Vision, Siemens Medical Solutions, Erlangen, Germany). The imaging protocols comprised SE T1w, TSE T2/PD w, FLAIR, DWI, and DTI sequences as well as a fully flow compensated 3D gradient-echo (GRE) sequence originally designed for generating conventional SWI contrast (TE/TR/FA=40ms/60ms/25°, voxel size=0.5×0.5×2 mm³; acquisition time=8-10 min) [6]. Temporal aliasing of the GRE phase was resolved using a special Laplacian operator [7]. Background phase contributions were eliminated with the SHARP technique [2]. A novel QSM algorithm (homogeneity enabled incremental dipole inversion, HEIDI [8]) was employed to yield quantitative susceptibility maps without streaking artifacts. Finally, the conventional MR contrasts were registered to the susceptibility maps using FLIRT [9] for ease of comparison. All data processing was carried out fully automatically using the Medical Computation Server [10].

RESULTS – Susceptibility maps provided additional information not obtained from conventional MR sequences in all of the 14 cases, in which either hemorrhage, calcification, or both were found. Three cases are presented here exemplarily. **Patient A** (male, 7 yrs 10 mos) suffered from tuberous sclerosis (Bourneville-Pringle disease, OMIM 191100) (Fig. 1), an inherited disease, characteristically showing subependymal nodules and dysplastic areas of the pallium (tubera), both of which may calcify. The FLAIR sequence showed hypointense lesions adjacent to both the caudate nuclei and the right trigonum. Further characterization of the lesions was not possible on the standard clinical MR contrasts (Fig. 1a, b). The conspicuous areas appeared strongly hypointense on the susceptibility map, indicating clearly substantial calcification. The structure of the lesions was much better delineated with QSM and few additional small calcifications were identified (arrows in Fig. 1c; mean magnetic susceptibilities between -0.3 and -0.15 ppm). Since tubera, sometimes not detectable with conventional MRI sequences, can be sources of seizures, detection of each tuber is important. **Patient B** (male, 10 yrs 2 mos) suffered from spontaneous bleeding of the right basal ganglia (straight arrows in Fig. 2). The hemorrhage was seen on the conventional MR images as a hypointense rim and an iso- to hypointense center on both T1-weighted (Fig. 2a) and GRE magnitude images (Fig. 2b). In addition, a subventricular clot (squared-ended arrows in Fig. 2) and intraventricular blood sedimentations (circle-ended arrows in Fig. 2) were identified on the GRE magnitude image (Fig. 2b). All lesions appeared hypointense on the susceptibility maps, confirming the presence of blood products. Interestingly, the hemorrhage of the basal ganglia was much more paramagnetic in the center (mean 1.1 ppm) compared to the periphery (mean 0.17 ppm), indicating resorption of blood products. The hypointense rim demarcating the bleeding represents an artifact, which can be explained by the strong field gradient in the vicinity of the lesion. **Patient C** (male, 2 yrs 7 mos) survived a severe traumatic brain injury after a fall from 6 m height. In this case, MRI was performed 6 months and 12 months after the initial injury. The susceptibility maps of both examinations (Fig. 3a, b) delineated several smaller blood collections (circle-ended arrow; mean susceptibility 0.3 ppm) and calcifications (straight arrows; mean susceptibility -0.35 ppm) of and adjacent to the dura mater. The largest, yet discrete, calcification was confirmed on CT (107 Hounsfield units (HU); Fig. 3c), performed six weeks after the traumatic event. While the dura appeared both isointense and slightly hyperintense on the susceptibility map in the initial MRI (squared-ended arrow in Fig. 3a), it showed hypointense signal on the susceptibility map acquired six months later (squared-ended arrow in Fig. 3b), indicating calcification of the dura and, thus, incomplete blood removal.

DISCUSSION – The presented clinical study clearly illustrates the potential of Quantitative Susceptibility Mapping (QSM) in pediatric neuroradiology, even at 1.5 T. Due to its high specificity, in particular with regard to differentiating between calcium and blood deposits, QSM represents a major addition to the neuroimaging toolbox with several important implications for routine applications. First, this new method is able to detect even minute hemorrhages and smallest calcifications, due to its intrinsic sensitivity. Moreover, acquisition of thin (1-2 mm) slices is not degraded by image noise. Second, as yet, there has been no MRI technique being able to differentiate reliably between calcification and hemorrhage. As to now, only CT can rather reliably differentiate between these entities. Due to the well known ionizing radiation risks, diagnostic imaging of children and adolescents should apply non-ionizing imaging methods whenever possible. Noninvasive differentiation between hemorrhage and calcification is important and necessary under certain medical conditions: Knowing the age of a hemorrhage may direct treatment options and is of great value in identifying the time point of a traumatic impact in cases of non-accidental injuries in infants. Presence of calcification may also help to classify brain tumors. Moreover, deposition of iron and calcium in unusual areas, such as brain parenchyma, may indicate rare, inherited metabolic diseases. Future studies on larger patient cohorts are certainly needed to explore the full potential of quantitative magnetic susceptibility for improved detection and characterization of lesions.

REFERENCES – [1] Li L and Leigh JS. 2004 *Magn Reson Med*. 51:1077-82. [2] Schweser F et al., 2011. *NeuroImage*. 54:2789-807. [3] Schäfer A et al., 2011. *Hum Brain Mapp* (in press) [4] Reichenbach JR and Haacke EM., 2001 *NMR Biomed*. 14:453-67. [5] Schweser F et al., 2010. *Med Phys*. 37:5165-78. [6] Reichenbach JR et al., 1997. *Radiology* 204:272-7. [7] Schofield MA and Zhu Y. *Optic Lett*. 2003;28(14):1194-6. [8] submitted to ISMRM 2012. [9] Jenkinson M. et al., 2002. *NeuroImage* 17, 825–41. [10] Lehr BW et al., 2011. *ISMRM* #2553.

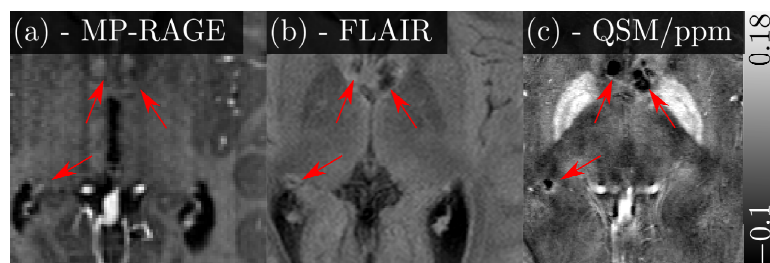


FIGURE 1. Patient A with bilateral calcified lesions adjacent to the caudate nucleus and right trigonum (arrows). Post Gd MP-RAGE and non-enhanced FLAIR image are shown in (a) and (b). All lesions were hypointense on the susceptibility map indicating substantial (diamagnetic) calcification.

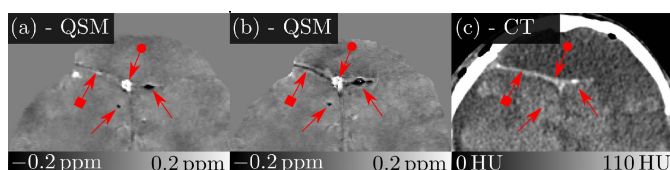


FIGURE 3. Patient C with posttraumatic evolution of a bifrontal hygroma. The first examination is shown in (a), the second examination, six months later, is shown in (b). Computed tomography (CT; six weeks after injury) confirmed discrete calcification (right straight arrow in (c)). Comparison of (a) and (b) indicates calcification of the dura mater in the follow-up examination.

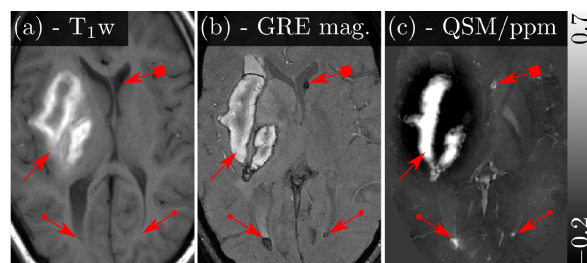


FIGURE 2. Patient B with hemorrhage into basal ganglia. Non-enhanced T1-weighted image (a), GRE magnitude image (b), susceptibility map (c).